Investigation of the meson-meson interaction

Yuheng Wu,[1,*] Xin Jin,[1,†] Hongxia Huang,[1,‡] Jialun Ping,[1,§] and Xinmei Zhu[2,‖]
[1]*Department of Physics, Nanjing Normal University, Nanjing, Jiangsu 210097, China*
[2]*Department of Physics, Yangzhou University, Yangzhou 225009, China*

(Received 6 October 2021; revised 17 June 2022; accepted 2 August 2022; published 22 August 2022)

In the framework of the quark delocalization color screening model, we investigate the meson-meson interaction in the four-quark system with the three flavors u, d, and s. The calculation of the effective potentials of all the S-wave states shows that for most states the interaction between two vector mesons is attractive, the one between a pseudoscalar meson and a vector meson is repulsive or weakly attractive, and the one between two pseudoscalar mesons is always repulsive. However, there are still some exceptions. The interaction of the $IJ = 00\ \pi\pi$ channel is attractive, while the one of the $IJ = 02\ \phi\phi$ channel is repulsive. So it is difficult to use the S-wave $\phi\phi$ state to explain the $X(2239)$ at present calculation. The S-wave $\rho\rho$ states are more likely to be resonance states, which are worthy of investigating in future work. The study of the contribution of each interaction term shows that both the one-gluon exchange and the kinetic energy interaction are important in the interaction between two mesons. The study of the variation of the delocalization parameter indicates that the contribution of the kinetic energy relates to the intermediate-range attraction mechanism in the quark delocalization color screening model (QDCSM), which is achieved by the quark delocalization.

DOI: 10.1103/PhysRevC.106.025204

I. INTRODUCTION

The study of the hadron-hadron interaction is one of the most active frontiers. The study of nucleon-nucleon (NN) interaction has lasted over seventy years. The quantitative description of NN interaction has been achieved in the one-boson-exchange models, the chiral perturbation theory, and quark models. The study of $\pi\pi$ interaction is also a classical subject in the field of strong interactions. The $\pi\pi$ scattering process has been studied as an important test of the strong interaction.

With the increasing experimental information of the meson spectrum, it becomes more and more important to develop a consistent understanding of the observed mesons from a theoretical point of view. For the low-lying vector and pseudoscalar mesons, this has been done quite successfully within the simple quark model by assuming the mesons to be quark-antiquark ($q\bar{q}$) states. For the scalar mesons, however, some questions still remain to be answered. One of the most noteworthy issues is the nature of the experimentally observed mesons $f_0(980)$ and $a_0(980)$. In a long-standing controversial discussion, the $f_0(980)$ has been described as a conventional $q\bar{q}$ meson [1], a $K\bar{K}$ molecule [2–4], or a tetraquark state [5]. In 2018, the BESIII Collaboration reported the observation of $a_0(980)$-$f_0(980)$ mixing [6], which would improve the understanding of the nature of $f_0(980)$ and $a_0(980)$.

In 2019, the BESIII Collaboration analyzed the cross section of the $e^+e^- \to K^+K^-$ process in the center-of-mass energy range from 2.00 to 3.08 GeV. A resonant structure $X(2239)$ was observed, which has a mass of $2239.2 \pm 7.1 \pm 11.3$ MeV and a width of $139.8 \pm 12.3 \pm 20.6$ MeV [7]. This state aroused the interest of theoretical physicists, and it has been studied extensively. Reference [8] investigated the mass spectrum of the $ss\bar{s}\bar{s}$ tetraquark states within the relativized quark model, and found that the $X(2239)$ can be assigned as a P-wave 1^{--} $ss\bar{s}\bar{s}$ tetraquark state. Reference [9] assigned the $X(2239)$ to be a hidden-strange molecular state from $\Lambda\bar{\Lambda}$ interaction.

Quantum chromodynamics(QCD) is the basic theory describing the strong interaction. However, the low-energy physics of QCD, such as the structure of hadrons, hadron-hadron interactions, and so on, is difficult to calculate directly from QCD, because of the nonperturbative complication. Lattice QCD has provided numerical results describing quark confinement between two static colorful quarks, a preliminary picture of the QCD vacuum, and the internal structure of hadrons, in addition to a phase transition of strongly interacting matter. Besides, the Hadron Spectrum Collaboration has presented a lattice QCD study of some meson-meson interactions, such as isoscalar $\pi\pi$, $K\bar{K}$, $\eta\eta$ scattering [10,11] and $\pi\omega$, $\pi\phi$ scattering [12]. Various QCD-inspired quark models have been developed to get physical insights into the

*191002007@njnu.edu.cn
†181002005@njnu.edu.cn
‡Corresponding author: hxhuang@njnu.edu.cn
§Corresponding author: jlping@njnu.edu.cn
‖zxm_yz@126.com

hadron-hadron interaction and multiquark systems. There are the cloudy bag model [13], MIT bag model [14], the Skyrme topological soliton model [15], the Friedberg-Lee nontopological soliton model [16], the constituent quark model [17,18], etc. Different models use quite different effective degrees of freedom, which might be indicative of the nature of low-energy QCD.

Among many phenomenological models, the quark delocalization color screening model (QDCSM) was developed in the 1990s with the aim of explaining the similarities between nuclear (hadronic clusters of quarks) and molecular forces [19]. In this model, the intermediate-range attraction is achieved by the quark delocalization, which is like the electron percolation in molecules. The color screening provides an effective description of the hidden color channel coupling [20], and leads to the possibility of the quark delocalization. The QDCSM gives a good description of NN and YN interactions and the properties of the deuteron [21]. It is also employed to calculate the baryon-baryon scattering phase shifts and predict the dibaryon candidates d^* [22] and $N\Omega$ [23]. Besides, it has been used for a systematic search of dibaryon candidates in the u, d, and s three-flavor world [24], and the law of baryon-baryon interaction was proposed. In QDCSM, the interaction between two decuplet baryons is always deeply attractive, the one between a decuplet baryon and an octet baryon is always weakly attractive, and the one between two octet baryons is mostly repulsive or weakly attractive. So it is interesting to extend this model to the study of the meson-meson interaction, which will help us to understand the low-energy physics of QCD and explore the nature of the new hadron states.

The structure of this paper is as follows. A brief introduction of the quark model and wave functions is given in Sec. II. Section III is devoted to the numerical results and discussions. The summary is given in Sec. IV.

II. MODEL AND WAVE FUNCTIONS

A. The quark delocalization color screening model (QDCSM)

The quark delocalization color screening model (QDCSM) has been described in detail in Refs. [19,21]. Here, we only give the Hamiltonian, in which three types of quark-quark interacting potentials are included. The first is the color confining potential, and it mimics the "confinement" property of QCD. The second is the one-gluon exchange (OGE) potential, reflecting the "asymptotic freedom" property of QCD, and the third is Goldstone boson exchange (OBE), coming from "chiral symmetry spontaneous breaking" of QCD in the low-energy region. The models with inclusion of these three types of potentials have been successfully applied to describe hadron spectra and hadron-hadron interactions [21,22].

To avoid double counting, two cutoffs are used in OBE. One is the sharp cutoff, which eliminates the short range contribution of OBE completely. Another is the soft cutoff, the form factor that is inserted into OBE, which makes the effects of OBE continuous. In Ref. [25], the one-pion exchange (OPE) with sharp cutoff and OGE interactions were used in studying nucleon-nucleon interactions. Our group make a comparison of these two cutoffs in Ref. [26], where the properties of the deuteron were well reproduced by inclusion of an OPE interaction in the QDCSM. By adjusting parameters, the binding energy and even the D-wave mixing of the deuteron can be reproduced well by both kinds of OPE, although the root-mean-square radius of the deuteron is a little smaller by using the Yukawa smearing in OPE. This indicates that the double counting effect of adding both OGE and OPE can be reduced by adjusting the parameters:

$$H = \sum_{i=1}^{4}\left(m_i + \frac{p_i^2}{2m_i}\right) - T_{CM} + \sum_{j>i=1}^{4}\left(V_{ij}^{\rm CON} + V_{ij}^{\rm OGE} + V_{ij}^{\rm OBE}\right), \tag{1}$$

$$V_{ij}^{\rm CON} = \begin{cases} -a_c\boldsymbol{\lambda}_i^c\cdot\boldsymbol{\lambda}_j^c\left(r_{ij}^2 + a_{ij}^0\right) & \text{if } i,j \text{ are in the same cluster,} \\ -a_c\boldsymbol{\lambda}_i^c\cdot\boldsymbol{\lambda}_j^c\left(\frac{1-e^{-\mu_{ij}r_{ij}^2}}{\mu_{ij}} + a_{ij}^0\right) & \text{otherwise,} \end{cases} \tag{2}$$

$$V_{ij}^{\rm OGE} = \frac{1}{4}\alpha_s\boldsymbol{\lambda}_i^c\cdot\boldsymbol{\lambda}_j^c\left[\frac{1}{r_{ij}} - \frac{\pi}{2}\delta(\boldsymbol{r}_{ij})\left(\frac{1}{m_i^2} + \frac{1}{m_j^2} + \frac{4\boldsymbol{\sigma}_i\cdot\boldsymbol{\sigma}_j}{3m_im_j}\right) - \frac{3}{4m_im_jr_{ij}^3}S_{ij}\right], \tag{3}$$

$$V_{ij}^{\rm OBE} = V_\pi(r_{ij})\sum_{a=1}^{3}\lambda_i^a\cdot\lambda_j^a + V_K(r_{ij})\sum_{a=4}^{7}\lambda_i^a\cdot\lambda_j^a + V_\eta(r_{ij})\left[\left(\lambda_i^8\cdot\lambda_j^8\right)\cos\theta_P - \left(\lambda_i^0\cdot\lambda_j^0\right)\sin\theta_P\right], \tag{4}$$

$$V_\chi(r_{ij}) = \frac{g_{ch}^2}{4\pi}\frac{m_\chi^2}{12m_im_j}\frac{\Lambda_\chi^2}{\Lambda_\chi^2 - m_\chi^2}m_\chi\left\{(\boldsymbol{\sigma}_i\cdot\boldsymbol{\sigma}_j)\left[Y(m_\chi\, r_{ij}) - \frac{\Lambda_\chi^3}{m_\chi^3}Y(\Lambda_\chi\, r_{ij})\right]\right.$$
$$\left. + \left[H(m_\chi r_{ij}) - \frac{\Lambda_\chi^3}{m_\chi^3}H(\Lambda_\chi r_{ij})\right]S_{ij}\right\}, \quad \chi = \pi, K, \eta, \tag{5}$$

$$S_{ij} = \left\{3\frac{(\boldsymbol{\sigma}_i\cdot\boldsymbol{r}_{ij})(\boldsymbol{\sigma}_j\cdot\boldsymbol{r}_{ij})}{r_{ij}^2} - \boldsymbol{\sigma}_i\cdot\boldsymbol{\sigma}_j\right\}, \tag{6}$$

$$H(x) = (1 + 3/x + 3/x^2)Y(x), \quad Y(x) = e^{-x}/x, \tag{7}$$

where S_{ij} is quark tensor operator; $Y(x)$ and $H(x)$ are standard Yukawa functions; T_{CM} is the kinetic energy of the center of mass; α_s is the quark-gluon coupling constant; and g_{ch} is the coupling constant for chiral field, which is determined from the $NN\pi$ coupling constant through

$$\frac{g_{ch}^2}{4\pi} = \left(\frac{3}{5}\right)^2 \frac{g_{\pi NN}^2}{4\pi} \frac{m_{u,d}^2}{m_N^2}. \tag{8}$$

The other symbols in the above expressions have their usual meanings. All model parameters, which are determined by fitting the meson spectrum, are from our previous work on the tetraquark $X(2900)$ [27]. A phenomenological color screening confinement potential is used here, and μ_{ij} is the color screening parameter, which is determined by fitting the deuteron properties, NN scattering phase shifts, and $N\Lambda$ and $N\Sigma$ scattering phase shifts, with $\mu_{uu} = 0.45$ fm^{-2}, $\mu_{us} = 0.19$ fm^{-2}, and $\mu_{ss} = 0.08$ fm^{-2}, satisfying the relation $\mu_{us}^2 = \mu_{uu}\mu_{ss}$.

B. Wave function

The resonating group method (RGM) [28] can be used to study a bound-state or a scattering problem. The wave function of the four-quark system is of the form

$$\Psi_{4q} = \mathcal{A}\sum_L \left[[\Psi_A\Psi_B]^{[\sigma]IS} \bigotimes \chi_L(\mathbf{R})\right]., \tag{9}$$

The symbol $\mathcal{A}$ is the antisymmetrization operator. $[\sigma] = [222]$ gives the total color symmetry, except that all other symbols have the usual meanings. Ψ_A and Ψ_B are the two-quark cluster wave functions,

$$\Psi_A = \left(\frac{1}{2\pi b^2}\right)^{3/4} e^{-\boldsymbol{\rho}_A^2/(4b^2)} \eta_{I_AS_A}\chi_A^c, \tag{10}$$

$$\Psi_B = \left(\frac{1}{2\pi b^2}\right)^{3/4} e^{-\boldsymbol{\rho}_B^2/(4b^2)} \eta_{I_BS_B}\chi_B^c, \tag{11}$$

Where $\eta_{I_AS_A}$ and $\eta_{I_BS_B}$ represent the multiplied wave functions of flavor and spin of the clusters A and B. χ_A^c and χ_B^c are the internal color wave functions of clusters A and B, and the Jacobi coordinates are

$$\begin{aligned} \boldsymbol{\rho}_A &= \mathbf{r}_1 - \mathbf{r}_2, & \boldsymbol{\rho}_B &= \mathbf{r}_3 - \mathbf{r}_4, \\ \mathbf{R}_A &= \tfrac{1}{2}(\mathbf{r}_1 + \mathbf{r}_2), & \mathbf{R}_B &= \tfrac{1}{2}(\mathbf{r}_3 + \mathbf{r}_4), \\ \mathbf{R} &= \mathbf{R}_A - \mathbf{R}_B, & \mathbf{R}_C &= \tfrac{1}{2}(\mathbf{R}_A + \mathbf{R}_B), \end{aligned}$$

From the variational principle, after variation with respect to the relative motion wave function $\chi(\mathbf{R}) = \sum_L \chi_L(\mathbf{R})$, one obtains the RGM equation

$$\int H(\mathbf{R},\mathbf{R}')\chi(\mathbf{R}')d\mathbf{R}' = E\int N(\mathbf{R},\mathbf{R}')\chi(\mathbf{R}')d\mathbf{R}', \tag{12}$$

where $H(\mathbf{R},\mathbf{R}')$ and $N(\mathbf{R},\mathbf{R}')$ are Hamiltonian and norm kernels. By solving the RGM equation, we can get the energies E and the wave functions. In fact, it is not convenient to work with the RGM expressions. So, we use the Gaussian bases to expand the relative motion wave function $\chi(\mathbf{R})$, respectively:

$$\chi_L(\boldsymbol{R}) = \frac{1}{\sqrt{4\pi}}\sum_L \left(\frac{1}{\pi b^2}\right)^{\frac{3}{4}} \sum_i C_{i,L} \times \int e^{-\frac{1}{2}(\boldsymbol{R}-\boldsymbol{S}_i)^2/b^2} Y_{LM}(\hat{\boldsymbol{S}}_i)d\hat{\boldsymbol{S}}_i. \tag{13}$$

where $\mathbf{S_i}$ is the generating coordinate in the model, denoting the separation of two reference centers. $\mathbf{R}$ is the dynamic coordinate defined in Eq. (12). In each cluster, the reference center is fixed, and the quarks move around the reference center, whereas the dynamic coordinate $\mathbf{R}$ is a quantity varies with the motion of each quark. $C_{i,L}$ is the expansion coefficient. After the inclusion of the center of mass motion,

$$\Phi_C(\boldsymbol{R}_C) = \left(\frac{4}{\pi b^2}\right)^{3/4} e^{-2\boldsymbol{R}_C^2/b^2}, \tag{14}$$

the ansatz, Eq. (9), can be rewritten as

$$\Psi_{4q} = \mathcal{A}\sum_{i,L} C_{i,L}\int \frac{d\Omega_{S_i}}{\sqrt{4\pi}} \prod_{\alpha=1}^{2}\phi_\alpha(\boldsymbol{S}_i)\prod_{\beta=3}^{4}\phi_\beta(-\boldsymbol{S}_i) \times\left[\left[\eta_{I_AS_A}\eta_{I_BS_B}\right]^{IS}Y_{LM}(\boldsymbol{S}_i)\right]^J\left[\chi_A^c\chi_B^c\right]^{[\sigma]}, \tag{15}$$

where $\phi_\alpha(\boldsymbol{S}_i)$ and $\phi_\beta(-\boldsymbol{S}_i)$ are the single-particle orbital wave functions with different reference centers:

$$\begin{aligned} \phi_\alpha(\boldsymbol{S}_i) &= \left(\frac{1}{\pi b^2}\right)^{3/4} e^{-\frac{1}{2}(\boldsymbol{r}_\alpha - \boldsymbol{S}_i/2)^2/b^2}, \\ \phi_\beta(-\boldsymbol{S}_i) &= \left(\frac{1}{\pi b^2}\right)^{3/4} e^{-\frac{1}{2}(\boldsymbol{r}_\beta + \boldsymbol{S}_i/2)^2/b^2}, \end{aligned} \tag{16}$$

With the reformulated ansatz, the RGM equation (13) becomes an algebraic eigenvalue equation:

$$\sum_{j,L} C_{j,L}H_{i,j}^{L,L'} = E\sum_j C_{j,L'}N_{i,j}^{L'}, \tag{17}$$

where $N_{i,j}^{L'}$ and $H_{i,j}^{L,L'}$ are the overlaps and Hamiltonian matrix elements (without the summation over L'), respectively. By solving the generalized eigenproblem, we can obtain the energies of the four-quark systems E and corresponding expansion coefficient $C_{j,L}$. Besides, the overlaps and Hamiltonian matrix elements can be used to calculate the effective potential. The effective potential between two mesons is defined as $V(S_i) = E(S_i) - E(\infty)$, where $E(S_i)$ is the energy of the system with the separation S_i of two reference centers, $E(S_i) = H_{i,i}/N_{i,i}$, where $N_{i,i}$ and $H_{i,i}$ are the overlaps and Hamiltonian matrix elements with the separation S_i.

In QDCSM, the quark delocalization is achieved by writing the single-particle orbital wave function as a linear combination of the left and right Gaussian functions, the single particle orbital wave functions used in the ordinary quark cluster model,

$$\begin{aligned} \psi_\alpha(\mathbf{S}_i, \epsilon(\mathbf{S}_i)) &= [\phi_\alpha(\mathbf{S}_i) + \epsilon(\mathbf{S}_i)\phi_\alpha(-\mathbf{S}_i)]/N(\epsilon(\mathbf{S}_i)), \\ \psi_\beta(-\mathbf{S}_i, \epsilon(\mathbf{S}_i)) &= [\phi_\beta(-\mathbf{S}_i) + \epsilon(\mathbf{S}_i)\phi_\beta(\mathbf{S}_i)]/N(\epsilon(\mathbf{S}_i)), \\ N(\epsilon(\mathbf{S}_i)) &= \sqrt{1 + \epsilon^2(\mathbf{S}_i) + 2\epsilon(\mathbf{S}_i)e^{-s_i^2/4b^2}}, \end{aligned} \tag{18}$$

For each separation S_i, the energies of the system are different for different ϵ, and the variational parameter ϵ is fixed according to the principle of minimum of energy, which can make the system choose the favorable configuration in the interacting process. So $\epsilon(\mathbf{S}_i)$ is determined variationally by the dynamics of the multiquark system itself rather than an adjustable parameter.

The flavor, the spin, and the color wave functions are constructed differently depending on different structures. Here, we investigate the meson-meson interaction, so we construct these wave functions within the meson-meson structure. As the first step, we give the wave functions of the meson cluster. The flavor wave functions of the meson cluster are

$$\chi^1_{I_{11}} = u\bar{d}, \quad \chi^2_{I_{1-1}} = -d\bar{u}, \quad \chi^3_{I_{10}} = \sqrt{\tfrac{1}{2}}(d\bar{d} - u\bar{u}),$$
$$\chi^4_{I_{\frac{1}{2}\frac{1}{2}}} = s\bar{d}, \quad \chi^5_{I_{\frac{1}{2}\frac{1}{2}}} = u\bar{s}, \qquad \chi^6_{I_{00}} = s\bar{s},$$

where the superscript of the χ is the index of the flavor wave function for a meson, and the subscript stands for the isospin I and the third component I_z. The spin wave functions of the meson cluster are

$$\chi^1_{\sigma_{11}} = \alpha\alpha, \quad \chi^2_{\sigma_{10}} = \sqrt{\tfrac{1}{2}}(\alpha\beta + \beta\alpha),$$
$$\chi^3_{\sigma_{1-1}} = \beta\beta, \quad \chi^4_{\sigma_{00}} = \sqrt{\tfrac{1}{2}}(\alpha\beta - \beta\alpha) \tag{19}$$

and the color wave function of a meson is

$$\chi^1_{[111]} = \sqrt{\tfrac{1}{3}}(r\bar{r} + g\bar{g} + b\bar{b}). \tag{20}$$

Then, the wave functions for the four-quark system with the meson-meson structure can be obtained by coupling the wave functions of two meson clusters. Every part of the wave functions are shown below. The flavor wave functions are

$$\psi^{f_1}_{22} = \chi^1_{I_{11}}\chi^1_{I_{11}}, \quad \psi^{f_2}_{\frac{3}{2}\frac{3}{2}} = \chi^1_{I_{11}}\chi^5_{I_{\frac{1}{2}\frac{1}{2}}}, \quad \psi^{f_3}_{\frac{1}{2}\frac{1}{2}} = \chi^6_{I_{00}}\chi^5_{I_{\frac{1}{2}\frac{1}{2}}}$$
$$\psi^{f_4}_{11} = \sqrt{\tfrac{1}{2}}\left[\chi^1_{I_{11}}\chi^3_{I_{10}} - \chi^3_{I_{10}}\chi^1_{I_{11}}\right],$$
$$\psi^{f_5}_{00} = \sqrt{\tfrac{1}{3}}\left[\chi^1_{I_{11}}\chi^2_{I_{1-1}} - \chi^3_{I_{10}}\chi^3_{I_{10}} + \chi^2_{I_{1-1}}\chi^1_{I_{11}}\right]. \tag{21}$$

The spin wave functions are

$$\psi^{\sigma_1}_{00} = \chi^4_{\sigma_{00}}\chi^4_{\sigma_{00}},$$
$$\psi^{\sigma_2}_{00} = \sqrt{\tfrac{1}{3}}\left[\chi^1_{\sigma_{11}}\chi^3_{\sigma_{1-1}} - \chi^2_{\sigma_{10}}\chi^2_{\sigma_{10}} + \chi^3_{\sigma_{1-1}}\chi^1_{\sigma_{11}}\right],$$
$$\psi^{\sigma_3}_{11} = \chi^4_{\sigma_{00}}\chi^1_{\sigma_{11}}, \quad \psi^{\sigma_4}_{11} = \chi^1_{\sigma_{11}}\chi^4_{\sigma_{00}},$$
$$\psi^{\sigma_5}_{11} = \sqrt{\tfrac{1}{2}}\left[\chi^1_{\sigma_{11}}\chi^2_{\sigma_{10}} - \chi^2_{\sigma_{10}}\chi^1_{\sigma_{11}}\right],$$
$$\psi^{\sigma_6}_{22} = \chi^1_{\sigma_{11}}\chi^1_{\sigma_{11}}. \tag{22}$$

The color wave function is

$$\psi^{c_1} = \chi^1_{[111]}\chi^1_{[111]}. \tag{23}$$

Finally, multiplying the wave functions ψ^L, ψ^σ, ψ^f, and ψ^c according to the definite quantum number of the system, we can acquire the total wave functions.

TABLE I. Channels for different systems.

I J	Channel
0 0	$\pi\pi$, $\eta\eta$, $\eta\eta'$, $\eta'\eta'$, $K\bar{K}$, $\phi\phi$, $\omega\omega$, $\omega\phi$, $\rho\rho$, $K^*\bar{K}^*$
0 1	$\pi\rho$, $\eta\phi$, $\eta\omega$, $\eta'\phi$, $\eta'\omega$, KK^*, $K\bar{K}^*$, $\bar{K}K^*$, $\omega\phi$, K^*K^*, $K^*\bar{K}^*$
0 2	$\phi\phi$, $\omega\omega$, $\rho\rho$, $\omega\phi$, $K^*\bar{K}^*$
1 0	$\pi\eta$, $\pi\eta'$, KK, $K\bar{K}$, $\omega\rho$, $\phi\rho$, K^*K^*, $K^*\bar{K}^*$
1 1	$\pi\rho$, $\pi\phi$, $\pi\omega$, $\eta\rho$, $\eta'\rho$, KK^*, $K\bar{K}^*$, $\bar{K}K^*$, $\omega\rho$, $\phi\rho$, $\rho\rho$, $K^*\bar{K}^*$
1 2	$\omega\rho$, $\phi\rho$, K^*K^*, $K^*\bar{K}^*$
2 0	$\pi\pi$, $\rho\rho$
2 1	$\pi\rho$
2 2	$\rho\rho$
$\frac{1}{2}$ 0	πK, $\pi\bar{K}$, ηK, $\eta\bar{K}$, $\eta' K$, $\eta'\bar{K}$, ϕK^*, $\phi\bar{K}^*$, ωK^*, $\omega\bar{K}^*$, ρK^*, $\rho\bar{K}^*$
$\frac{1}{2}$ 1	πK^*, $\pi\bar{K}^*$, ρK, $\rho\bar{K}$, ηK^*, $\eta\bar{K}^*$, $\eta' K^*$, $\eta'\bar{K}^*$, ωK, $\omega\bar{K}$, ϕK, $\phi\bar{K}$, ωK^*, $\omega\bar{K}^*$, ϕK^*, $\phi\bar{K}^*$, ρK^*, $\rho\bar{K}^*$
$\frac{1}{2}$ 2	ϕK^*, $\phi\bar{K}^*$, ωK^*, $\omega\bar{K}^*$, ρK^*, $\rho\bar{K}^*$
$\frac{3}{2}$ 0	πK, $\pi\bar{K}$, ρK^*, $\rho\bar{K}^*$
$\frac{3}{2}$ 1	πK^*, $\pi\bar{K}^*$, ρK, $\rho\bar{K}$, ρK^*, $\rho\bar{K}^*$
$\frac{3}{2}$ 2	ρK^*, $\rho\bar{K}^*$

III. THE RESULT AND DISCUSSION

In this work, we investigate the interaction between two light mesons, which includes three types: two pseudoscalar mesons (PP), a pseudoscalar meson and a vector meson (PV), and two vector mesons (VV). As a preliminary calculation, only the S-wave systems are studied here, so we set the orbital angular momentum to zero. Due to the limit of the spin quantum number, the PP system has the total spin quantum number $S = 0$, the PV system has the total spin quantum number $S = 1$, while the VV system has three possible spin quantum numbers, which are $S = 0$, 1, and 2. Since the orbital angular momentum is $L = 0$, the total angular momentum can be $J = 0$ for PP systems, $J = 0$ and 1 for PV systems, and $J = 0$, 1, and 2 for VV systems. The isospin of the four-quark systems with light quarks can be $I = 0$, $\frac{1}{2}$, 1, $\frac{3}{2}$, and 2. All possible channels for different systems are listed in Table I.

To investigate the interaction between two mesons, we calculate the effective potentials of all the channels listed in Table I. All the results are shown in Figs. 1–7. Here, we note that some channels have the same effective potential. For example, the potentials of the πK and $\pi\bar{K}$ are the same, because the contribution of each interaction term to the πK and $\pi\bar{K}$ is the same. To save space, we only show the potential for one of them in the figure. And the same treatment is used in similar situations.

For the $I = 0$ system, there are five PP channels and five VV channels for the system with $J = 0$. It is clear that Fig. 1(a) shows the effective potential between PP mesons, while Fig. 1(b) shows the effective potential between VV mesons. We can see that the potential is repulsive for the $\eta\eta$, $\eta\eta'$, $\eta'\eta'$, and $K\bar{K}$ channels, while it is attractive for the $\pi\pi$ channel. In contrast, the potential is attractive for all channels of the VV systems. The attraction between ρ-ρ is the largest one, followed by that of the $\omega\omega$ channel, which is larger than that of the $\omega\phi$ channel. Besides, the attraction of both the $\phi\phi$ and $K^*\bar{K}^*$ channels is very weak. For the $J = 1$ system,

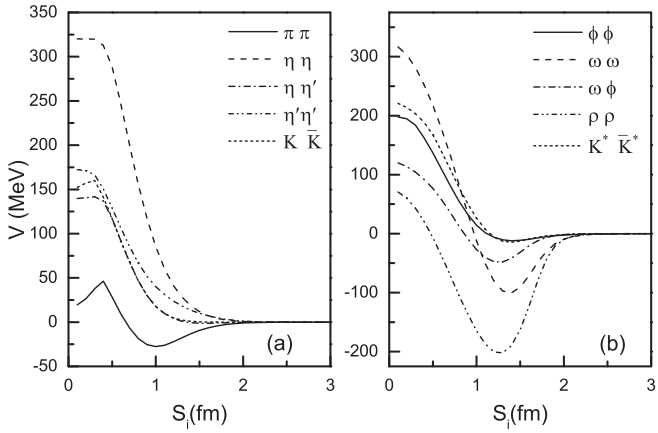

FIG. 1. Figures (a) and (b) are the effective potentials of all channels for the system with $IJ = 00$.

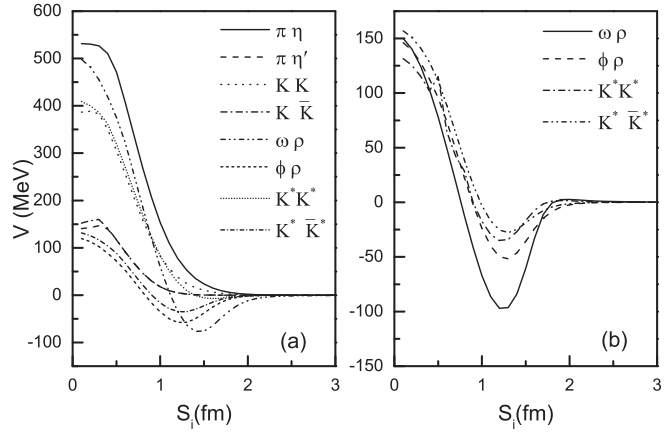

FIG. 3. Figure (a) is the effective potentials of all channels for the system with $IJ = 10$, and (b) is for the system with $IJ = 12$.

there are seven PV channels and three VV channels. From Figs. 2(a) and 2(b) we can see that the potential for the $\eta'\phi$, $\eta\omega$, and $K\bar{K}^*$ channels is repulsive, while the one for other channels is attractive. In addition, the attraction of the VV channels is a little deeper than that of the PV channels. For the $J = 2$ system, there are five VV channels. It is obvious in Fig. 2(c) that there is a deep attraction between two ρ mesons. The potential for all channels is attractive, except for the $\phi\phi$ channels.

For the $I = 1$ system, there are four PP channels and four VV channels for the system with $J = 0$. From Fig. 3(a) we can see that the potential for the four VV channels is all attractive, while it is repulsive for the four PP channels. Moreover, there are four VV channels for the system with $J = 2$, and the potential of all of them is attractive, which is shown in Fig. 3(b). For the system with $J = 1$, there are seven PV channels and four VV channels, and the potential of them is shown in Fig. 4. The potential for the PV channels $\pi\omega$ and $\eta\rho$ is repulsive, while it is attractive for the PV channels $\pi\rho$ and $\eta'\rho$. Besides, there is a very shallow attraction for the PV channels $\pi\phi$, KK^*, and $K\bar{K}^*$. By contrast, the potential for all VV channels is attractive, and that for both $\omega\rho$ and $\rho\rho$ channels is very deep.

For the $I = 2$ system, it is obvious in Fig. 5 that the potential for both the $\pi\pi$ channel with $J = 0$ and $\pi\rho$ channels with $J = 1$ is repulsive, while the one for the $\rho\rho$ channel with $J = 0$ and $J = 2$ is attractive.

For the $I = \frac{1}{2}$ system, Fig. 6(a) shows the potential for three PP channels and three VV channels with $J = 0$. One sees that the potential is repulsive for two PP channels ηK and $\eta' K$, while it is attractive for the πK channel. Moreover, it is obviously attractive for three VV channels. Figure 6(b) shows the potential for six PV channels and three VV channels with $J = 1$, from which we can see that the potential is repulsive for four PV channels ηK^*, $\eta' K^*$, ωK, and ϕK. However, the potential is attractive for other PV channels πK^* and ρK. It is also attractive for all VV channels. Meanwhile, Fig. 6(c) shows the potential for three VV channels with $J = 2$. Obviously, the potential for both the ωK^* and ρK^* is attractive, while it is repulsive for the ϕK^* channel.

For the $I = \frac{3}{2}$ system, Fig. 7 clearly shows that the potential is attractive for the VV channel $\rho\bar{K}^*$ with $J = 0$, 1 and 2.

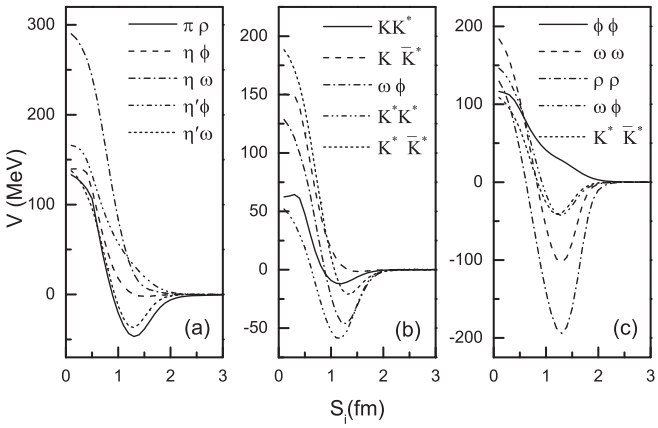

FIG. 2. Figures (a) and (b) are the effective potentials of all channels for the system with $IJ = 01$, and (c) is for the system with $IJ = 02$.

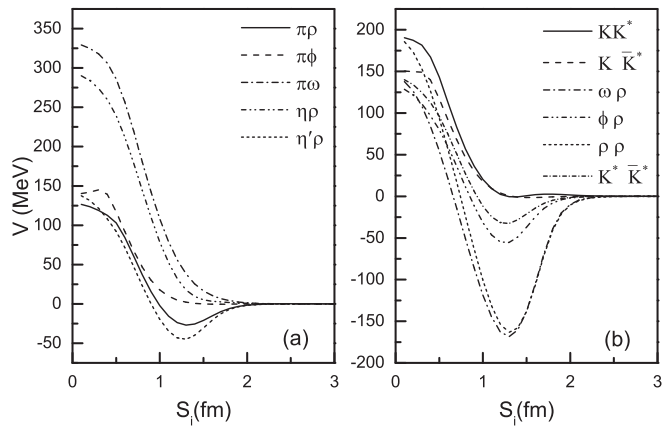

FIG. 4. Figures (a) and (b) are the effective potentials of all channels for the system with $IJ = 11$.

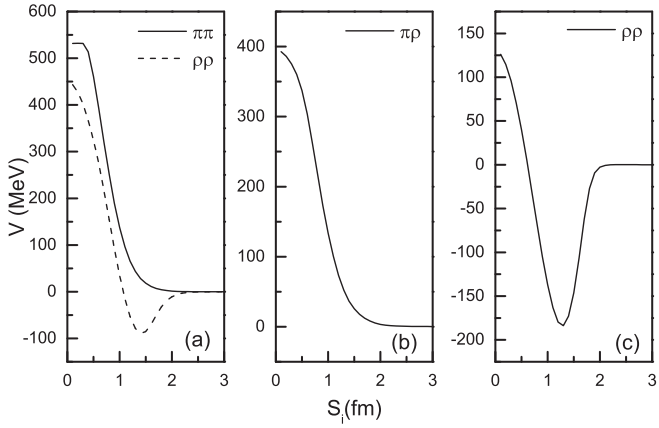

FIG. 5. Figure (a) is the effective potentials of all channels for the system with $IJ = 20$, (b) is for the system with $IJ = 21$, and (c) is for the system with $IJ = 22$.

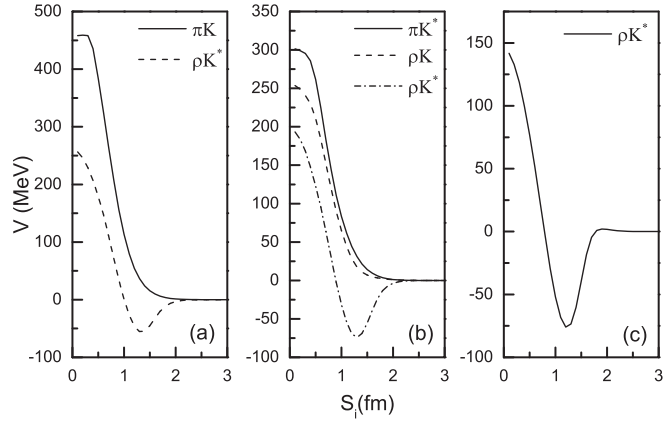

FIG. 7. Figure (a) is the effective potentials of all channels for the system with $IJ = \frac{3}{2}0$, (b) is for the system with $IJ = \frac{3}{2}1$, and (c) is for the system with $IJ = \frac{3}{2}2$.

However, there is no attractive potential for either the PP channel πK with $J = 0$ or the PV channels πK^* and ρK with $J = 1$.

From the above analysis, it is not difficult to find a rule that for most channels the interaction between two vector mesons is attractive, the one between a pseudoscalar meson and a vector meson is repulsive or weakly attractive and the one between two pseudoscalar mesons is always repulsive. This law is similar to the one of the baryon-baryon interaction. In Ref. [24], the interaction between two decuplet baryons is always deeply attractive, the one between a decuplet baryon and an octet baryon is always weakly attractive, and the one between two octet baryons is mostly repulsive or weakly attractive. However, there are still some exceptions. For example, the potential for the PP channel $\pi\pi$ with $IJ = 00$ is attractive, while it is repulsive for the $\pi\pi$ with $IJ = 20$. This conclusion is consistent with most theoretical work. The $\pi\pi$ interaction has been studied as an important test of the strong interaction for a long time. Much attention has been paid to the isospin $I =]$ $\pi\pi$ S-wave interaction due to its direct relation to the σ particle and the scalar glueball candidates [29–35]. However, the study of the $I = 2$ $\pi\pi$ S-wave interaction is also necessary since a correct description of the $I = 2$ $\pi\pi$ S-wave interaction is important for the extraction of the $I = 0$ $\pi\pi$ S-wave interaction from experimental data [36]. Moreover, the S-wave $\phi\phi$ channel is a special state, which is composed of two vector mesons but with the repulsive interaction. So it is difficult to use the S-wave $\phi\phi$ state to explain the $X(2239)$ in the present calculation. To explore the candidate of $X(2239)$, the study of the high partial wave of the $\phi\phi$ state will be performed in future work.

To further study the $\pi\pi$ and $\phi\phi$ interactions, we calculate the scattering phase shifts of the S-wave $\pi\pi$ and $\phi\phi$ channels by using the well-developed Kohn-Hulthen-Kato (KHK) variational method. The details of the method can be found in Ref. [28]. The phase shifts of the S-wave $\pi\pi$ and $\phi\phi$ channels are shown in Figs. 8 and 9, respectively. From Fig. 8 we can see that the scattering phase shift of the $\pi\pi$ channel with $IJ = 00$ goes to 180 degrees at the incident energy

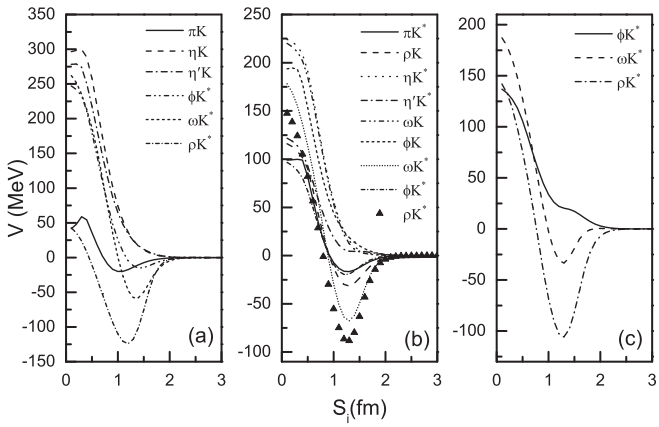

FIG. 6. Figure (a) is the effective potentials of all channels for the system with $IJ = \frac{1}{2}0$, (b) is for the system with $IJ = \frac{1}{2}1$, and (c) is for the system with $IJ = \frac{1}{2}2$.

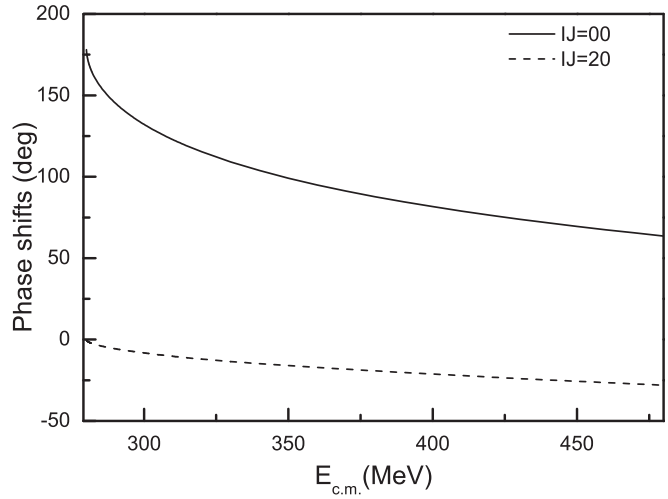

FIG. 8. The scattering phase shifts of $\pi\pi$ channels with $IJ = 00$ and $IJ = 20$.

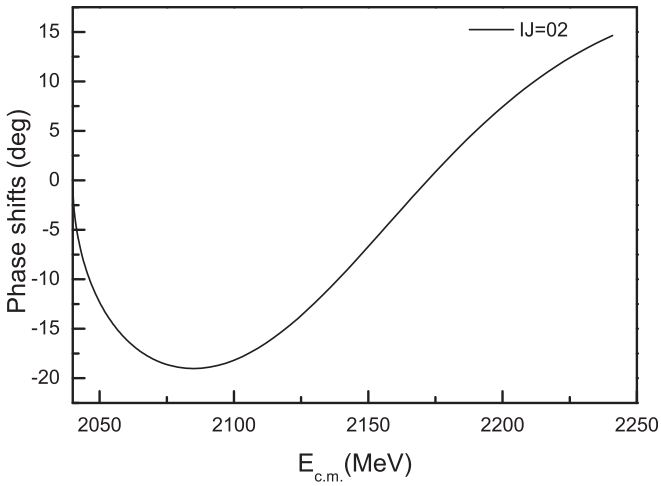

FIG. 9. The scattering phase shifts of $\phi\phi$ channel with $IJ = 02$.

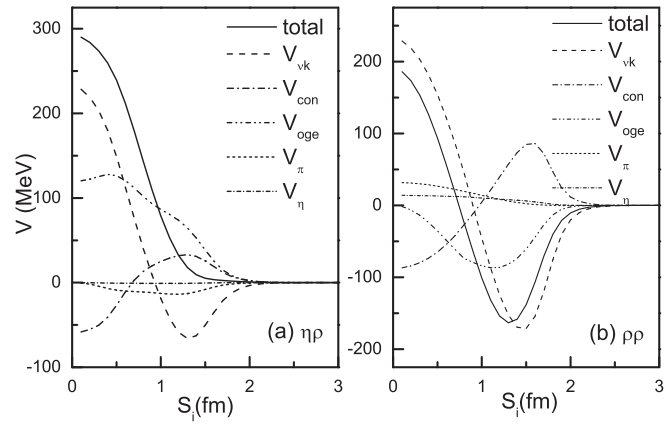

FIG. 10. The contributions to the effective potentials from various terms of $\eta\rho$ and $\rho\rho$ with $IJ = 11$.

$E_{\text{c.m.}} \approx 280$ and rapidly decreases as $E_{\text{c.m.}}$ increases, which implies the existence of a bound state for this channel. This is consistent with the work of using lattice QCD by the Hadron Spectrum Collaboration [11]. Besides, the phase shift of this channel is positive, which indicates that the interaction of the $IJ = 00$ $\pi\pi$ channel is attractive, and this is consistent with the attractive behavior of the effective potential of this channel. However, it is inconsistent with the experimental data. This may be due to the complexity of the π system. In the work of Ref. [37], the authors employed the effective Lagrangian and Roy equation to study the $\pi\pi$ phase shift, and the $I = 0$ S-wave phase shift is found to be increasing, roughly linearly, from threshold, which is consistent with the experimental data. In their work, π represents the corresponding Goldstone boson. In our work, on the one hand we treat the π meson as the $q\bar{q}$ ($q = u$ or d) system when studying the $\pi\pi$ interaction, but on the other hand we regard π as the Goldstone boson in the OPE interaction. It is still a debatable problem to regard the π meson as the $q\bar{q}$ system. Besides, it is also a complex system for the tetraquark, which may involve many factors, such as the mixing of two- and four-quark systems (sea quarks/antiquarks excitation), σ resonance, etc. These factors may need to be taken into account in future study.

From Fig. 8, we can see that the phase shifts of the $\pi\pi$ channel with $IJ = 20$ are negative, which means that the interaction of the $IJ = 20$ $\pi\pi$ channel is repulsive, and this is also consistent with the repulsive behavior of the effective potential of this channel. Moreover, the phase shifts of the $IJ = 02$ $\phi\phi$ channel shown in Fig. 9 also indicate the repulsive interaction for this channel. We will explain why the interaction is repulsive between two ϕ mesons later.

In addition, the deep attraction between two vector mesons also attracts great attention to the systems composed of two vector mesons. For the S-wave $\rho\rho$ state, the deepest effective attraction of the states with different quantum numbers is from about 100 to 200 MeV. We find that the attraction of the state with isospin $I = 0$ is larger than that with $I = 2$. For the $I = 0$ $\rho\rho$ the attraction of the state with the angular momentum $J = 0$ is larger than that with $J = 2$, while for the $I = 2$ $\rho\rho$ the attraction of the state with $J = 0$ is smaller than that with $J = 2$. Nevertheless, there is great attraction in the $\rho\rho$ state, which makes it more possible to form some bound states or resonance states.

In order to explore the contribution of each interaction term to the system, the interaction from various terms, the kinetic energy ($V_{\nu k}$) [$\sum \frac{p_i^2}{2m_i} - T_{CM}$ in Eq. (1)], the confinement (V_{con}), the one-gluon exchange (V_{oge}), and the one-boson exchange (V_π, V_K, V_η), are studied. One may note that all these interactions are the energies between two mesons. To save space, we take a few states as examples: the $\eta\rho$ and $\rho\rho$ states with $IJ = 11$ and the $\pi\pi$ and $\rho\rho$ states with $IJ = 20$. The contribution of each interaction term is shown in Figs. 10 and 11. From Fig. 10 we can see that the kinetic energy term provides an attractive interaction for both $IJ = 11$ $\eta\rho$ and $\rho\rho$ states, and this attraction of the $\rho\rho$ state is obviously larger than that of the $\eta\rho$ state. Besides, the one-gluon exchange interaction provides deep attraction for the $\rho\rho$ state, while it is repulsive for the $\eta\rho$ state. In contrast, the contribution of other items is small. So both the kinetic energy and the one-gluon exchange

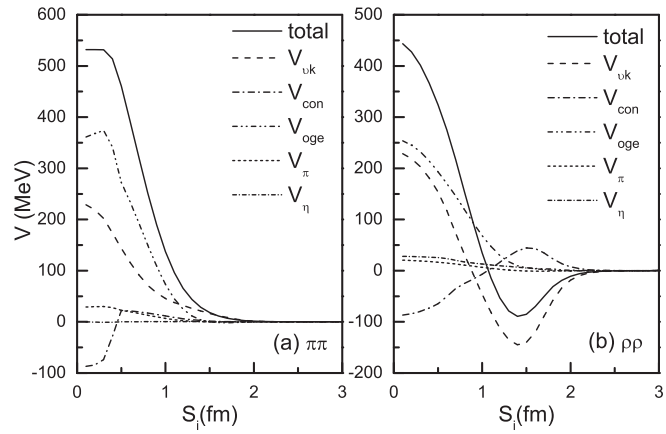

FIG. 11. The contributions to the effective potentials from various terms of $\pi\pi$ and $\rho\rho$ with $IJ = 20$.

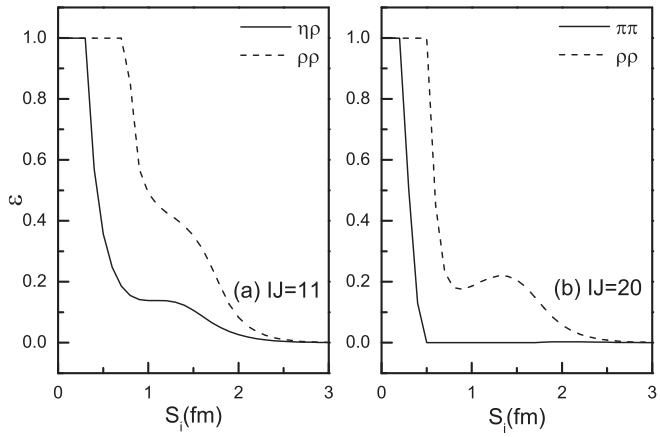

FIG. 12. The delocalization parameter ε of $\eta\rho$ and $\rho\rho$ with $IJ = 11$ and of $\pi\pi$ and $\rho\rho$ with $IJ = 20$.

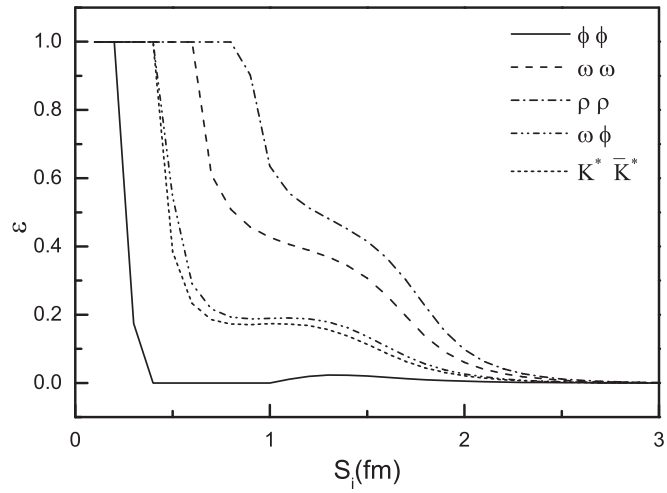

FIG. 13. The delocalization parameter ε for the $IJ = 02$ system.

interactions provide attraction, which leads a large total attraction for the $\rho\rho$ state, while for the $\eta\rho$ the repulsive interaction by the one-gluon exchange and the attractive interaction by the kinetic energy almost cancel each other out, which result in the total repulsive interaction. Towards the $\pi\pi$ and $\rho\rho$ states with $IJ = 20$, we find that the one-gluon exchange provides repulsive interaction for both $\pi\pi$ and $\rho\rho$ states. However, the kinetic energy interaction is attractive for the $\rho\rho$ state, which leads to a total attraction, while it is repulsive for the $\pi\pi$ state, which leads to a total repulsive interaction. From the above discussion, we can see that the kinetic energy interaction plays an important role in providing attractions, which relates to the intermediate-range attraction mechanism in QDCSM.

In QDCSM, two ingredients were introduced: quark delocalization and color screening; the former is to enlarge the model variational space to take into account the mutual distortion or the internal excitations of nucleons in the course of interaction, and the latter is assuming that the quark-quark interaction dependents on quark states and aims to take into account the QCD effect which has not been included in the two body confinement and effective one gluon exchange yet. By introducing the quark delocalization, quarks have larger motion space, and the kinetic energy of the system will be depressed compared with two noninteracting mesons. So it is possible for the kinetic energy to provide an attractive potential in QDCSM. Therefore, in this model, the intermediate-range attraction is achieved by the quark delocalization, which is like the electron delocalization in molecules. The color screening is needed to make the quark delocalization effective. It is worth noting that the delocalization parameter is not an adjusted one but determined variationally by the dynamics of the system itself. Here, we show the variation of the delocalization parameter, which relates to the intermediate-range attraction for the different states.

In Fig. 12(a), the delocalization parameter of the $\rho\rho$ state with $IJ = 11$ is close to 1 when the distance S between two mesons is less than 0.8 fm, which means that the quarks are likely to run between different clusters, thereby reducing the kinetic energy and introducing the attractive interaction. In contrast, the delocalization parameter of the $\eta\rho$ state with $IJ = 11$ approaches 1 when $S \leqslant 0.3$ fm, and it quickly approaches 0 as the distance increases. Although it can also reduce the kinetic energy, the reduction of the $\eta\rho$ state is not as great as that of the $\rho\rho$ state, so the attraction of the $\eta\rho$ state is smaller than that of the $\rho\rho$ state, as shown in Fig. 10. The case is similar for the $\pi\pi$ and $\rho\rho$ states with $IJ = 20$. From Fig. 12(b) we can see that the delocalization parameter of the $\rho\rho$ state with $IJ = 20$ is close to 1 when the distance $S \leqslant 0.5$ fm, then it approaches 0 more quickly than that of the $\rho\rho$ state with $IJ = 11$, which is why the kinetic energy of the $\rho\rho$ state with $IJ = 11$ is lower than that of the $\rho\rho$ state with $IJ = 20$. With regard to the $\pi\pi$ state with $IJ = 20$, the delocalization parameter is close to 1 only when the distance $S \leqslant 0.2$ fm, and it approaches 0 more quickly than that of the $\eta\rho$ state with $IJ = 11$, so the kinetic energy of $\pi\pi$ state with $IJ = 20$ is much higher than that of the $\eta\rho$ state with $IJ = 11$, even it cannot provide the attractive interaction.

The variation of the delocalization parameter can also be used to explain the repulsive interaction of the $\phi\phi$ state. We show the variation of the delocalization parameter for the $IJ = 02$ system in Fig. 13. Comparing the $\phi\phi$ and $\rho\rho$ states, although both of them are composed of two vector mesons, the quark component of the $\phi\phi$ state is $s\bar{s}s\bar{s}$, and the one of the $\rho\rho$ state is $q\bar{q}q\bar{q}$ ($q = u$ or d). The mass of the strange quark is heavier than that of the nonstrange quark, so the strange quark is less likely to run between two clusters. As shown in Fig. 13, the delocalization parameter of the $\phi\phi$ state is close to 1 only when the distance $S \leqslant 0.2$ fm, and it approaches to 0 very quickly, so it cannot reduce the kinetic energy too much. So the interaction between two ϕ is repulsive. By comparing Figs. 13 and 2(c), we find that the variation of the delocalization parameter relates to the interaction between two mesons. The more the quark runs between two mesons, the stronger the attraction is between the two mesons.

IV. SUMMARY

The study of the hadron-hadron interaction is one of the critical issues in hadron physics. In this work, we investigate the meson-meson interaction in the four-quark system with

the three flavors u, d, and s in the framework of the QDCSM. The effective potentials of all the S-wave states, the contribution of each interaction term to the states, as well as the variation of the delocalization parameter, which relates to the intermediate-range attraction for the different states, are all studied in this work.

Our results show that for most states the interaction between two vector mesons is attractive, the one between a pseudoscalar meson and a vector meson is repulsive or weakly attractive, and the one between two pseudoscalar mesons is always repulsive. However, there are still some exceptions. The interaction of the $IJ = 00$ $\pi\pi$ channel is attractive, while the one of the $IJ = 02$ $\phi\phi$ channel is repulsive. This law is similar to the one of the baryon-baryon interaction. In dibaryon systems, the interaction between two Δ baryons is deeply attractive, which leads to the well-known bound state d^*. So we should pay more attention to the four-quark system composed of two vector mesons here. Among all these states, the S-wave $\rho\rho$ state, especially the state with $IJ = 00$, is more likely to be a bound state or a resonance state. We will continue to study these states in further work. Moreover, the scattering phase shifts of the $\pi\pi$ channels with $IJ = 00$ and $IJ = 20$ and of the $\phi\phi$ channel with $IJ = 02$ are preliminary studied. To further study the meson-meson interaction and observe more resonance states, we will take a deeper look at the meson-meson scattering process in future work.

The study of the contribution of each interaction term shows that both the one-gluon exchange and the kinetic energy interaction play an important role in the interaction between two mesons and, the kinetic energy relates to the intermediate-range attraction mechanism in QDCSM, which is achieved by the quark delocalization. The delocalization parameter approaching 1 means that the quarks are more willing to run between the two mesons, thereby reducing the kinetic energy and introducing the attractive interaction. Our results show that the more the quark runs between two mesons, the stronger the attraction is between the two mesons.

In present work, our purpose is to study the S-wave meson-meson interactions and find out whether there are some rules for these interactions. The P-wave phase shift of $\pi\pi$ is usually mixed with the ρ resonance, because the ρ state is observed in the $\pi\pi$ scattering. The calculation by coupling with four-quark and two-quark systems is more complicated, which should be carried out by the unquenched quark model. So we do not do this calculation in present work, but it is work worth studying, and it is also the work we will do in the future.

ACKNOWLEDGMENTS

This work is supported partly by the National Natural Science Foundation of China under Contracts No. 11675080, No. 11775118, and No. 11535005.

[1] D. Morgan, Phys. Lett. B **51**, 71 (1974).
[2] J. Weinstein and N. Isgur, Phys. Rev. Lett. **48**, 659 (1982).
[3] J. Weinstein and N. Isgur, Phys. Rev. D **41**, 2236 (1990).
[4] J. Weinstein and N. Isgur, Phys. Rev. D **27**, 588 (1983).
[5] R. L. Jaffe, Phys. Rev. D **15**, 267 (1977).
[6] M. Ablikim *et al.* (BESIII Collaboration), Phys. Rev. Lett. **121**, 022001 (2018).
[7] M. Ablikim *et al.* (BESIII Collaboration), Phys. Rev. D **99**, 032001 (2019).
[8] Q. F. Lv, K. L. Wang, and Y. B. Dong, Chin. Phys. C **44**, 024101 (2020).
[9] J. T. Zhu, Y. Liu, D. Y. Chen, L. Y. Jiang, and J. He, Chin. Phys. C **44**, 123103 (2020).
[10] R. A. Briceño, J. J. Dudek, R. G. Edwards, and D. J. Wilson, Phys. Rev. Lett. **118**, 022002 (2017).
[11] R. A. Briceño, J. J. Dudek, R. G. Edwards, and D. J. Wilson, Phys. Rev. D **97**, 054513 (2018).
[12] A. J. Woss, C. E. Thomas, J. J. Dudek, R. G. Edwards, and D. J. Wilson, Phys. Rev. D **100**, 054506 (2019).
[13] A. W. Thomas, Adv. Nucl. Phys. **13**, 1 (1984); T. DeGrand, R. L. Jaffe, K. Johnson, and J. Kiskis, Phys. Rev. D **12**, 2060 (1975).
[14] A. Chodos, R. L. Jaffe, K. Johnson, C. B. Thorn, and V. F. Weisskofp, Phys. Rev. D **9**, 3471 (1974).
[15] T. H. R. Skyrme, Nucl. Phys. **31**, 556 (1962); E. Witten, Nucl. Phys. B **160**, 57 (1979); G. S. Adkins, C. R. Nappi, and E. Witten, *ibid.* **228**, 552 (1983).
[16] R. Friedberg and T. D. Lee, Phys. Rev. D **15**, 1694 (1977); **16**, 1096 (1977); **18**, 2623 (1978).
[17] A. De Rujula, H. Georgi, and S. L. Glashow, Phys. Rev. D **12**, 147 (1975).
[18] N. Isgur and G. Karl, Phys. Rev. D **18**, 4187 (1978); **19**, 2653 (1979); **20**, 1191 (1979).
[19] F. Wang, G. H. Wu, L. J. Teng, and T. Goldman, Phys. Rev. Lett. **69**, 2901 (1992).
[20] H. X. Huang, P. Xu, J. L. Ping, and F. Wang, Phys. Rev. C **84**, 064001 (2011).
[21] J. L. Ping, F. Wang, and T. Goldman, Nucl. Phys. A **657**, 95 (1999); G. H. Wu, J. L. Ping, L. J. Teng *et al.*, *ibid.* **673**, 279 (2000).
[22] J. L. Ping, H. X. Huang, H. R. Pang, F. Wang, and C. W. Wong, Phys. Rev. C **79**, 024001 (2009).
[23] H. X. Huang, J. L. Ping, and F. Wang, Phys. Rev. C **92**, 065202 (2015).
[24] F. Wang, J. L. Ping, G. H. Wu, L. J. Teng, and T. Goldman, Phys. Rev. C **51**, 3411 (1995).
[25] K. Maltman and N. Isgur, Phys. Rev. Lett. **50**, 1827 (1983).
[26] J. L. Ping, H. R. Pang, F. Wang, and T. Goldman, Phys. Rev. C **65**, 044003 (2002).
[27] Y. Y. Xue, X. Jin, H. X. Huang, J. L. Ping, and F. Wang, Phys. Rev. D **103**, 054010 (2021).
[28] M. Kamimura, Prog. Theor. Phys. Suppl. **62**, 236 (1977).
[29] C. Patrignani *et al.* (Particle Data Group), Chin. Phys. C **40**, 100001 (2016).
[30] P. Minkovski and W. Ochs, Eur. Phys. J. C **9**, 283 (1999).
[31] D. V. Bugg, A. V. Sarantsev, and B. S. Zou, Nucl. Phys. B **471**, 59 (1996).

[32] B. Ananthanarayan, G. Colangelo, J. Gasser, and H. Leutwyler, Phys. Rep. **353**, 207 (2001).
[33] V. V. Anisovich *et al.*, Phys. Lett. B **389**, 388 (1996).
[34] N. N. Achasov and G. N. Shestakov, Phys. Rev. D **67**, 114018 (2003).
[35] B. S. Zou and D. V. Bugg, Phys. Rev. D **48**, R3948 (1993).
[36] F. Q. Wu, B. S. Zou, L. Li, and D. V. Bugg, Nucl. Phys. A **735**, 111 (2004).
[37] G. Colangelo, J. Gasser, and H. Leutwyler, Nucl. Phys. B **603**, 125 (2001).